Appl Biochem Biotechnol (2010) 160:1896–1908
DOI 10.1007/s12010-009-8730-9

The Effect of Trifluoroethanol on Tyrosinase Activity and Conformation: Inhibition Kinetics and Computational Simulations

Zhi-Rong Lü · Long Shi · Jun Wang · Daeui Park · Jong Bhak · Jun-Mo Yang · Yong-Doo Park · Hong-Wei Zhou · Fei Zou

Received: 24 October 2008 / Accepted: 26 July 2009 /
Published online: 24 August 2009

Abstract We studied the inhibitory effects of trifluoroethanol (TFE) on the activity and conformation of tyrosinase. TFE increased the degree of secondary structure of tyrosinase, which directly resulted in enzyme inactivation. A reciprocal study showed that TFE inhibited tyrosinase in a slope-parabolic mixed-type inhibition manner (K_I=0.5±0.096 M). Time-interval kinetic studies showed that the inhibition was best described as first order with biphasic processes. Intrinsic and 1-anilinonaphthalene-8-sulfonate-binding fluorescences were also measured to gain more insight into the supposed structural changes; these showed that TFE induced a conspicuous tertiary structural change in tyrosinase by exposing hydrophobic surfaces. We also predicted the tertiary structure of tyrosinase and simulated its docking with TFE. The docking simulation was successful with significant scores (binding energy for Autodock4=−4.75 kcal/mol; for Dock6=−23.07 kcal/mol) and suggested that the TRP173 residue was mainly responsible for the interaction with TFE. Our results provide insight into the structure of tyrosinase and allow us to describe a new inhibition strategy that works by inducing conformational changes rather than targeting the active site of the protein.

Z.-R. Lü · L. Shi · Y.-D. Park · H.-W. Zhou (✉) · F. Zou (✉)
Department of Environmental Health, School of Public Health and Tropical Medicine,
Southern Medical University, Guangzhou 510515, People's Republic of China
e-mail: biodegradation@gmail.com
e-mail: zoufei_dean@hotmail.com

J. Wang
School of Medicine, Shenzhen University, Shenzhen 518060, People's Republic of China

D. Park · J. Bhak
Korean BioInformation Center (KOBIC), KRIBB, Daejeon 305-806, Korea

J.-M. Yang
Department of Dermatology, Sungkyunkwan University School of Medicine, Samsung Medical Center,
Seoul 135-710, Korea

Y.-D. Park
Yangtze Delta Region Institute, Tsinghua University, Jiaxing, 314050, People's Republic of China

Keywords Tyrosinase · Trifluoroethanol · Inhibition kinetics · Secondary structure · Docking simulation

Abbreviations

DOPA	3,4-Dihydroxyphenylalanine
TFE	2,2,2-Trifluoroethanol
ANS	1-Anilinonaphthalene-8-sulfonate
CD	Circular dichroism

Introduction

2,2,2-Trifluoroethanol (TFE) is well known as a cosolvent in protein-folding studies [1–3] and the detection of membrane proteins [4, 5]. TFE destabilizes tertiary and quaternary structures of proteins by disrupting hydrophobic interactions at low concentrations (5–20%) but stabilizes secondary structures such as α-helices and, to a lesser extent, β-sheet structures at higher concentrations (30%) [6–10]. The stabilization effect of TFE on secondary structure is due to TFE's ability to strengthen intrahelical hydrogen bonds and reinforce hydrogen bonds between carbonyl and amidic groups by removing water molecules in the proximity of the solute. In contrast, TFE can destabilize the protein structure and induces folding intermediates in some cases, thereby accelerating aggregation due to the promotion of hydrophobic interactions between amino acid side chains [11–13]. A previous computational simulation showed that coating peptides with TFE resulted in the removal of alternative hydrogen-bonding partners and induced the formation of intrapeptide hydrogen bonds due to a low dielectric environment [14]. TFE can therefore be considered to be a stabilizer for most enzymes; however, for some enzymes, TFE apparently acts as a denaturant resulting in disruption of the tertiary structure of the protein and loss of activity [15, 16]. An investigation into the mechanisms by which TFE modifies the secondary and tertiary structures of enzymes is therefore very important.

Tyrosinase (EC 1.14.18.1) is a critical enzyme that has multi-catalytic functions in the melanosynthetic pathway, and it is distributed ubiquitously in organisms. Two Cu^{2+} ions individually connected with three histidines at the active site are charged in their cupric or cuprous state and are directly involved in different catalytic reactions via the oxy-, deoxy-, and met-states [17, 18]. The tyrosinase catalysis mechanism is very complex as this enzyme can catalyze multiple reactions, and the mechanism therefore needs to be investigated from different sources using various kinetic methods. Because the crystallographic structure of tyrosinase has not yet been clearly solved, there is little data available to investigate structure–function relationships in this enzyme.

Tyrosinase deficiencies are directly associated with pigmentation disorders in mammals [19] and cause a browning effect in vegetables [20]. Tyrosinase also participates in cuticle formation in insects [21]. Therefore, regulation of the enzymatic activity of tyrosinase has been the focus of investigation due to its potential applications in medicine, cosmetics, and agriculture. There are very few reports of regulation of the enzymatic activity of tyrosinase via conformational changes. The major strategy for tyrosinase inhibition has been chelating of the copper ions at the active site. In this paper, we propose a new approach to tyrosinase inhibition: modulation of secondary and tertiary structures of tyrosinase directly involved with catalysis. We simulated the 3D structure of tyrosinase, evaluated its docking behavior with TFE, and investigated its putative binding residues (ASP169, ALA171, TRP173, PHE261, and ASP536 from Autodock4; PHE170 and TRP173 from DOCK6). Our results

provide insight into tyrosinase inhibition kinetics and the conformational changes induced by TFE.

Materials and Methods

Materials

Tyrosinase (MW 128 kDa), L-DOPA, TFE, and *N*-acetyl-L-tryptophan were purchased from Sigma. When L-DOPA was used as a substrate in our experiments, the purchased tyrosinase had a K_m=0.51±0.03 mM (V_{max}=0.3±0.01) which was evaluated using a Lineweaver–Burk plot.

Tyrosinase Assay

The assay for tyrosinase was performed spectrophotometrically [22]. Reactions were performed in a typical reaction volume of 1 ml to which 10 μl of enzyme solution was added to measure tyrosinase activity. The activity and absorption were measured with a Perkin Elmer Lambda Bio U/V spectrophotometer. The *v* value used in the present study indicates the change in absorbance at 492 nm per minute.

CD Spectroscopy

Circular dichroism (CD) spectra were recorded on a Jasco 725 spectropolarimeter. The sample cell path length was 22 mm. CD measurements were carried out as described previously [23, 24].

Kinetic Analysis for the Parabolic Mixed-Type Inhibition

According to the equations reported previously [25], the Lineweaver–Burk equation can be written as:

$$\frac{1}{v} = \frac{K_m}{V_{max}}\left[1 + \frac{[I]}{K_i}\right]\frac{1}{[S]} + \frac{1}{V_{max}}\left[1 + \frac{[I]}{\alpha K_i}\right] \tag{1}$$

and

$$Slope = \frac{K_m}{V_{max}} + \frac{K_m[I]}{V_{max}K_i} \tag{2}$$

K_I cannot be determined directly from the usual equations due to the parabolic relationship between *slope* versus [I], and thus Eq. (3), which is a modification of a previous report, was applied [26]:

$$\ln\left(\frac{1}{K_{Islope}}\right) = \frac{1}{K_I^2}[I] - \frac{2\beta}{K_I} \tag{3}$$

where the reciprocal of the $K_{I\ slope}$ is replotted versus the corresponding inhibitor. The replot has a slope of $1/K_I^2$ when there are multiple binding sites. In addition, β is the factor by which $K_{I\ slope}$ changes when the inhibitor occupies the enzyme.

Intrinsic and ANS-Binding Fluorescence Measurements

Fluorescence emission spectra were measured with a Jasco FP750 spectrofluorometer using a 1-cm-path-length cuvette. An excitation wavelength of 280 nm was used for the tryptophan fluorescence measurements, and the emission wavelength ranged between 300 and 410 nm. Changes in the extrinsic fluorescence intensity were studied by labeling with 40 μM ANS for 30 min prior to measurement. An excitation wavelength of 390 nm was used for the ANS-binding fluorescence, and the emission wavelength ranged from 400 to 520 nm.

Homology Modeling of Tyrosinase

A three-dimensional model of tyrosinase comprising 556 amino acids was built using MODELLER9v1 [27] based on homology modeling [28]. The MODELLER program automatically provides an all-atom model using alignments between the query sequence and known homologous structures. We retrieved the known homologous structures of tyrosinase from the Protein Data Bank (PDB) (http://www.pdb.org) and found that four entries (PDB entry=1wxc, 1xom, 2oic, 2oid) were suitable structural templates (average 26% sequence identity) and were partial tyrosinase homologs. A sequence alignment between tyrosinase and the templates was constructed by ALIGN2D in the MODELLER package. Based on the sequence alignment, the 3D structure of tyrosinase was constructed with a high level of confidence. We subsequently calculated the conformational energy of the structural model of tyrosinase using the discrete optimized protein energy (DOPE) score as a stability metric.

In silico Docking of Tyrosinase and TFE

Among the many tools available for *in silico* protein–ligand docking, AutoDock4 and DOCK6 are the ones most commonly used because of their automated docking capability. The programs both perform ligand docking using a set of predefined 3D grids of the target protein; however, AutoDock uses a random search technique [29] while DOCK uses a systemic search technique [30]. Therefore, we used two slightly different approaches to evaluate the docking of tyrosinase and TFE. The original structure of TFE was derived from the PubChem database (compound ID 6409) (http://www.pubchem.org) [31]. To prepare for the docking procedure, the following steps were taken: (1) conversion of 2D structures to 3D structures, (2) calculation of charges, (3) addition of hydrogen atoms, and (4) location of pockets. For these steps, we used the fconverter program of the J-Chem package (http://www.chemaxon.com/) and OpenBabel (http://openbabel.sourceforge.org).

In this study, all kinetic reactions and measurements were performed in 50 mM sodium phosphate buffer (pH 7.0).

Results

TFE-Induced Secondary Structural Changes of Tyrosinase Measured by CD

At a TFE concentration of less than 10%, the level of secondary structure increased slightly (Fig. 1a); however, as the concentration of TFE increased, the overall amount of secondary structure decreased gradually in a dose-dependent manner (Fig. 1b). Although TFE is

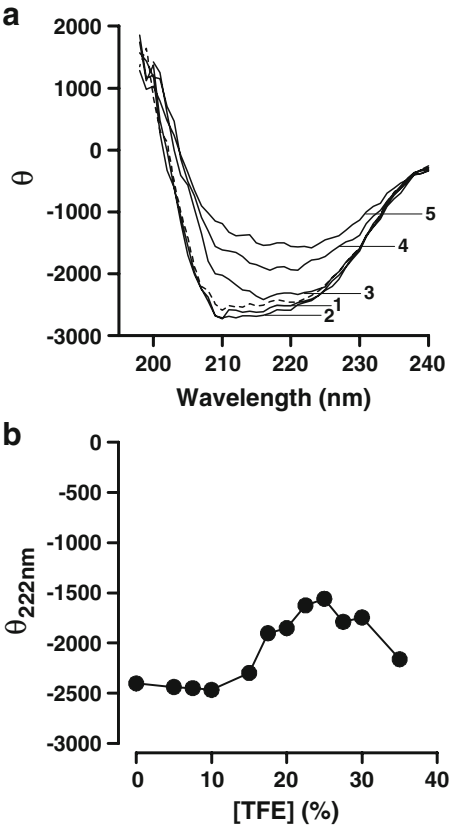

Fig. 1 CD spectra changes of tyrosinase in the presence of TFE. **a** Labels *1* to *5* indicate TFE concentrations of 5%, 10%, 15%, 20%, and 25%, respectively. (—) Control spectra (0% TFE). The final concentration of the enzyme was 4 μg/ml. **b** Data was collected at 222 nm of the CD spectra in the presence of various concentrations of TFE. Other conditions were the same as for (**a**)

known to stabilize helices within proteins, it actually decreased the extent of secondary structure in tyrosinase. Specifically, in the concentration range of 15% to 25% TFE, the spectrum of secondary structural changes decreased significantly, while at higher concentrations (25% to 35%) the spectrum of secondary structural changes increased. To elucidate the relationship between secondary structure changes and tyrosinase activity, we assayed the L-DOPA oxidase activity of tyrosinase in the presence of TFE.

Effect of TFE on the Activity of Tyrosinase: Inhibition and Inactivation Kinetics

At concentrations of TFE less than 10%, tyrosinase activity was sustained, and even slightly activated. When TFE concentrations were higher than 10%, however, tyrosinase activity gradually decreased in a dose-dependent manner (IC_{50}=21% or 2.9 M) (Fig. 2a). To assay the reversibility of TFE-mediated modification, plots of the remaining activity versus [E] were applied (Fig. 2b). The results showed straight lines passing through the origin, confirming that the inhibition by TFE was reversible. To evaluate the mode of inhibition, Lineweaver–Burk plot analysis was performed. The apparent V_{max} and K_m both appeared to change simultaneously (Fig. 3a), and a secondary replot of *slope* versus [I] yielded a parabolic curve (Fig. 3b) indicating that TFE induced a parabolic mixed-type inhibition. By using Eq. (3), the K_I value was calculated as 0.5±0.096 M (3.63±0.7%) and

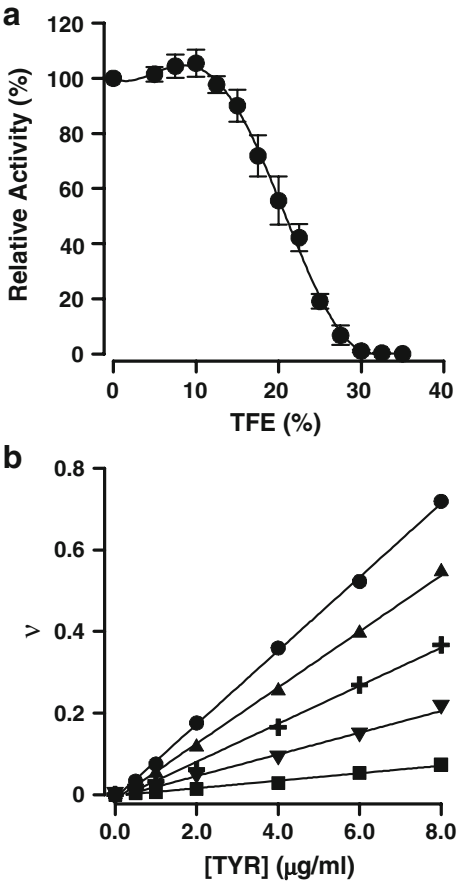

Fig. 2 Inhibitory effect of TFE on tyrosinase. **a** Inactivation of tyrosinase by TFE. Data and *bars* are presented as the mean ± standard deviation (n=3). Tyrosinase was incubated with various concentrations of TFE for 2 h and then added to the assay system. **b** Plots of v (enzyme activity) versus [E]. The TFE concentrations were 0 (●), 15% (▲), 20% (+), 22.5% (▼), and 25% (■). The final concentrations of L-DOPA and the enzyme were 2 mM and 4 μg/ml, respectively

the value of β was calculated as 1.09. In all, the experimental data fit very well to the predicted equations.

To evaluate the inactivation kinetics and rate constants, time-interval measurements were performed (Fig. 4). Enzyme activity was not inactivated in the presence of 10% TFE, and only when TFE was higher than 20% did activity gradually decrease in a time-dependent manner. This result is entirely consistent with the data presented in Fig. 1a, where the equilibrium state of the enzyme activity was not inactivated at less than 10% TFE. Subsequent kinetic analyses using semi-logarithmic plots showed biphasic inactivation, with fast (k_1) and slow (k_2) aspects (Fig. 5), where a monophasic process developed into a biphasic process as the concentration of TFE increased; the inhibition followed first-order kinetics. The microscopic inactivation rate constants are summarized in Table 1: inactivation occurred as a result of changes in the transition free-energy energy ($\Delta\Delta G^{\circ\prime}$), which decreased in a TFE concentration-dependent manner.

TFE-Induced Tertiary Structural Changes in Tyrosinase According to Fluorescence Spectra

Tertiary structural changes of tyrosinase in the presence of TFE were also measured (Fig. 6). We found that TFE induced a change in the intrinsic fluorescence spectra of

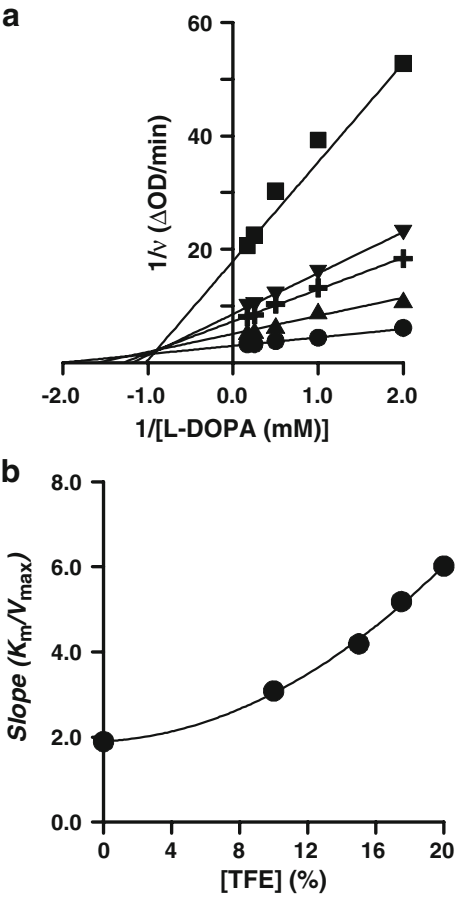

Fig. 3 Inhibition kinetics for tyrosinase in the presence of TFE. (**a**) Lineweaver–Burk plot. The TFE concentrations were 0 (●), 15% (▲), 17.5% (+), 20% (▼), and 22.5% (■). **b** The secondary replot of *Slope* (V_{max}/K_m) versus [TFE]. Data were collected from (**a**). The final enzyme concentration was 4 μg/ml

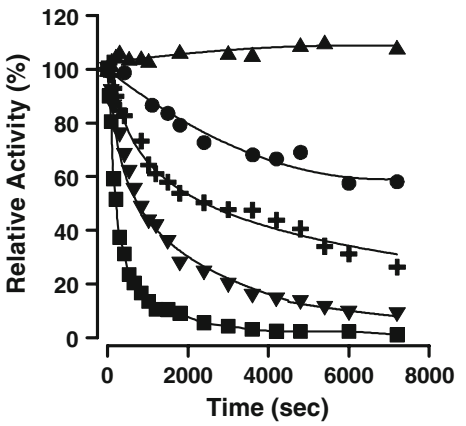

Fig. 4 Kinetic time courses for tyrosinase inactivation in the presence of TFE. The enzyme solutions were mixed with various concentrations of TFE: 10% (▲), 20% (●), 25% (+), 27.5% (▼), and 30% (■) and aliquots were taken at the indicated time intervals

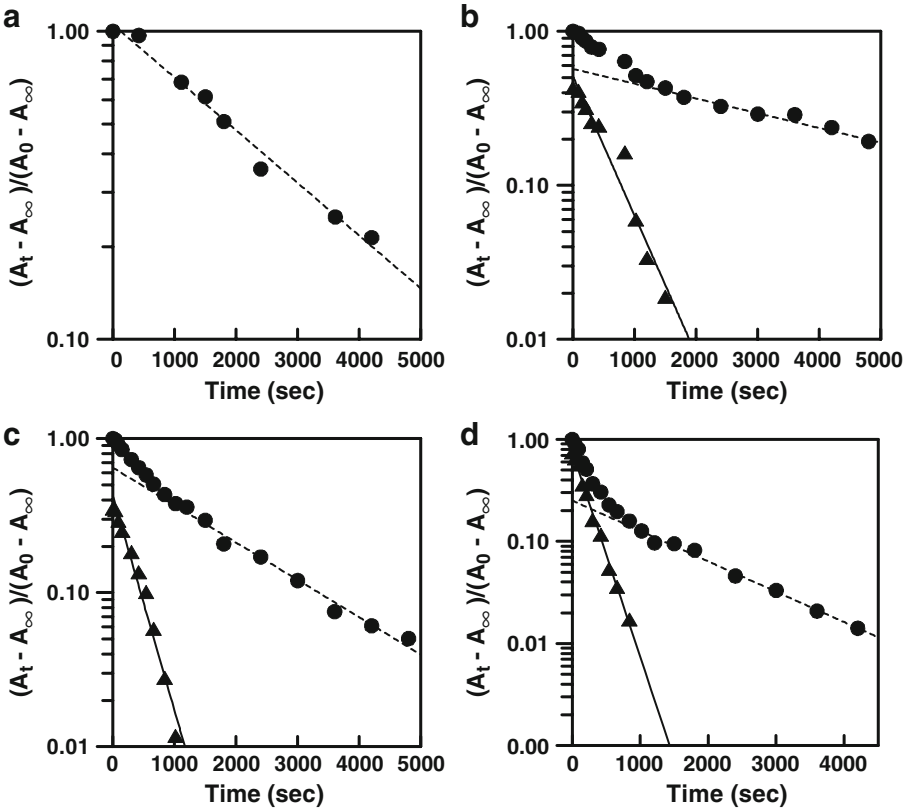

Fig. 5 Semi-logarithmic plot analyses. (●) Experimental points. (▲) Points obtained by subtracting the contribution of the slow phase from the data in the curve (—). Slopes of the curves (— or –) indicate the rate constants. The final concentrations of L-DOPA and the enzyme were 2 mM and 4 μg/ml, respectively

tyrosinase, which gradually decreased via a red-shift wavelength effect (Fig. 6a). A plot of maximum peak wavelength versus the concentration of TFE revealed a sigmoid relationship and indicated that TFE induces tertiary structural disruption of tyrosinase (Fig. 6b). We also monitored the ANS-binding fluorescence changes; the ANS-fluorescence spectra were significantly increased by TFE (Fig. 7a), indicating that hydrophobic surfaces of tyrosinase were exposed by TFE. In addition, the increase was dose dependent, as observed from a secondary replot (Fig. 7b). Tertiary structural changes resulting from modulation of the secondary structure modulation therefore appear to be directly associated with the observed changes in enzyme activity.

Computational Prediction of 3D Tyrosinase Structure and TFE Docking Simulation

Because the crystallographic structure of tyrosinase has not been elucidated, we selected template structures from the PDB entries 1wxc, 1xom, 2oic, and 2oid that have sequence identities of 25%, 29%, 26%, and 25% to tyrosinase, respectively, to simulate the 3D structure of tyrosinase. In the predicted structure of tyrosinase, we used the binding pocket expanded to a size of 496 $Å^3$, as indicated in yellow in Fig. 8. The docking between tyrosinase and TFE was successful with significant scores (−2.25 kcal/mol by Autodock4

Table 1 Microscopic inactivation rate constants of tyrosinase in the presence of TFE.

TFE (%)	Inactivation rate constants ($\times 10^{-3}$ s^{-1})[a]			Transition free-energy change (kJ/mol·min^{-1})[b]
	k_1	k_2	A	
20	–	–	0.39	29.59
25	2.07	0.22	–	25.45
27.5	3.20	0.55	–	24.37
30	4.62	0.68	–	23.46

[a] Data were calculated as shown in Fig. 5. k_1 and k_2 are the first-order rate constants for the fast and slow phases, respectively. *A* is for the monophasic rate constant

[b] According to Tams and Welinder [37] with slight modification, transition free-energy change per minute, $\Delta\Delta G^{\circ}=-RT\ln k$, where k is a time constant for the major phase of the inactivation reaction

and −14.36 kcal/mol by Dock6). Using Autodock4 and Dock6, we searched for TFE binding residues of tyrosinase that were close in distance. We found that the most important expected binding residues interacting with TFE were PHE170, THR175, VAL177, GLY251, PHE261, and ASP536 according to Autodock4, and GLU250 and ASP536 according to Dock6 (red box in Fig. 8); both programs identified ASP536. The docking

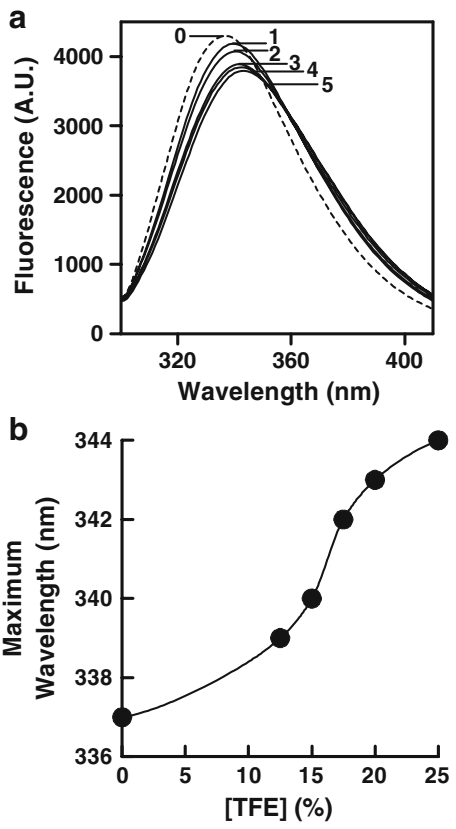

Fig. 6 Intrinsic fluorescence changes of tyrosinase in the presence of different concentrations of TFE. **a** Intrinsic fluorescence changes. Tyrosinase was incubated with TFE for 3 h before being measured. The curve (—) shows the native state. Labels *1* to *5* indicate TFE concentrations of 12.5%, 15%, 17.5%, 20%, and 25%, respectively. **b** Plot of maximum wavelength versus [TFE]. Data were obtained from (**a**)

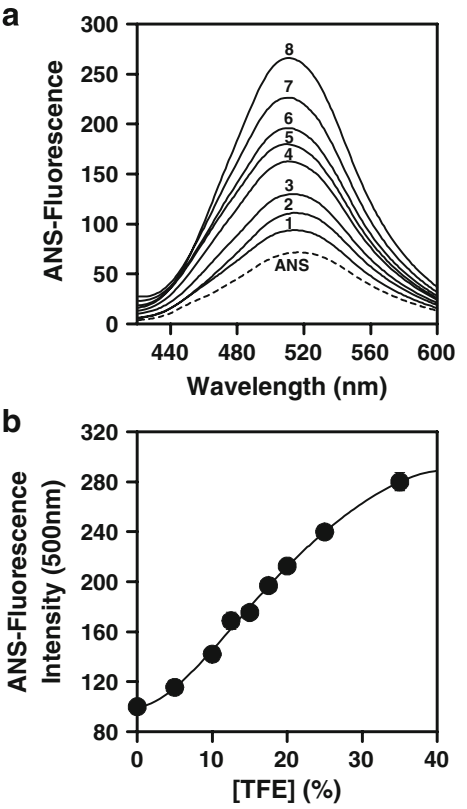

Fig. 7 ANS-binding fluorescence changes. **a** TFE concentrations labeled *1* to *8* are 0, 5%, 10%, 15%, 17.5%, 20%, 25%, and 35%, respectively. **b** Plot of the relative ANS-fluorescence intensity versus [TFE] at 500 nm. The data shown are mean values (n=2)

simulation provided supported for the slope-parabolic mixed-type inhibition observed, as this type of inhibition is generally observed when there are multiple binding sites for an inhibitor.

Discussion

Advances in biophysical techniques, both thermodynamic and kinetic, suggest the presence of stable intermediate conformational states of a number of proteins; these have made a critical contribution to our understanding of protein-folding phenomena. TFE is one of the most frequently applied denaturants used to study protein folding, and the effect of TFE on the activity of enzymes and on the stability of proteins has been well documented. Our data, which is consistent with the results of previous studies, provides further insight into the mechanism of TFE-induced changes in protein structure. We conducted both a real-time analysis as well as equilibrium kinetic unfolding studies of tyrosinase in the presence of TFE to expand our understanding of the structure of tyrosinase. Recently, Wei et al. reported that bovine carbonic anhydrase II is slightly activated in less than 10% TFE, but at higher TFE concentrations (greater than 15%), the enzyme becomes inactivated [32]. Similarly, as shown in Fig. 2a, tyrosinase was not inactivated by low concentrations of TFE, but rather, it was slightly activated. Therefore, TFE, regardless of structural changes,

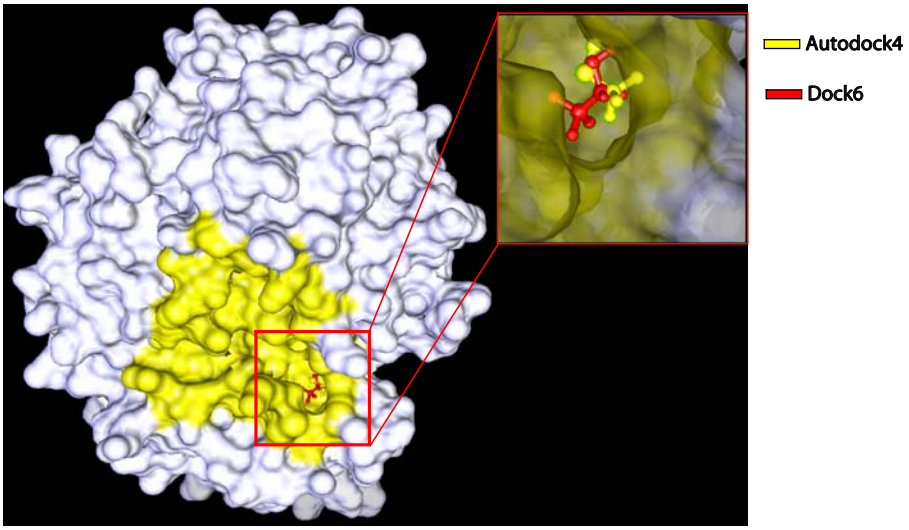

Fig. 8 Computational structure prediction for tyrosinase and docking simulation with TFE. Predicted 3D structure of mushroom tyrosinase. The *red box* indicates TFE binding sites with tyrosinase residues. The *yellow stick* is TFE docked by the Autodock4 program and the *red stick* is TFE docked by Dock6

stabilizes tyrosinase at low concentrations; however, higher concentrations of TFE (higher than 20%) acted as a denaturant as was expected.

We found that secondary and tertiary structural changes induced by TFE affected accessibility to the substrate; a complex type of inhibition was therefore identified. Our simulations indicated that TFE can form a ligand-binding complex directly with some residues of tyrosinase, and these amino acid residues are thought to be important for the docking of TFE at the first stage of folding. TFE induced an increased amount of helical structure in tyrosinase that served to disrupt this enzyme's overall tertiary structure, explaining how TFE can function as a denaturant. The partial conformational changes induced by TFE are likely to have affected the substrate-enzyme state of the parabolic V_{max} changes and, simultaneously, interfered with L-DOPA docking to the active site, resulting in K_m changes. Complex types of inhibition of tyrosinase by various compounds have been observed previously [25, 26, 33–35]. Compared to these results, however, the TFE-induced mechanism of inhibition was different in two major ways: TFE did not bind directly to the copper ions of the active site, and secondary structural changes were accompanied by tertiary structural changes that directly induced a complete loss of activity.

The shift from slight activation in the presence of low concentrations of TFE to monophasic inactivation in the presence of high TFE concentrations implies that tyrosinase transiently passes through several distinct intermediates until it reaches a completely unfolded state. Thus, the accumulation of intermediates as a result of increasing TFE concentration was likely responsible for the overall decrease in enzymatic activity. TFE docking to the enzyme occurred very quickly but only gradually induced the structural changes associated with the loss of activity, after which it transitioned to a slow phase. The partially unfolded states of transient intermediates underwent a slow inactivation until complete unfolding. This hypothesis was supported by thermodynamic calculations, which showed conspicuous decreases in transition free-energy changes ($\Delta\Delta G^{\circ}$) with increasing TFE concentration. Similar results have also been reported in a previous study where

tyrosinase was inactivated by denaturants such as urea, guanidine hydrochloride, and sodium dodecyl sulfate in a biphasic process [36]. The accumulation of intermediates indicates that tyrosinase has a stable tertiary structure.

Taken together, the results of our study suggest the following: (1) TFE ligand binding to tyrosinase causes a complex type of inhibition of enzymatic activity; (2) secondary structural changes of tyrosinase result in the exposure of hydrophobic surfaces; (3) the putative binding residues for TFE are predicted by computational docking simulation; (4) TFE inactivation of tyrosinase represents a novel strategy for inactivating tyrosinase and developing inhibitors. Our study provides greater insight into the role of amino acid residues within the binding pocket of tyrosinase and provides useful information regarding the 3D structure of tyrosinase. The inhibition kinetics combined with the computational prediction allowed us to elucidate structural changes in tyrosinase during catalysis in the presence of TFE.

Acknowledgements This study was supported by a grant from the National Basic Research Program of China (no. 2006CB504100). Dr. Yong-Doo Park was supported by fund from the Science and Technology Planning Project of Jiaxing (no. 2008AZ1024), Zhejiang. Dr. Jun-Mo Yang was supported by the grants of the Korea Health 21 R&D Project (Ministry of Health, Welfare and Family Affairs, Republic of Korea, 01-PJ3-PG6-01GN12-0001 and A030003).

References

1. Huang, K., Park, Y. D., Cao, Z. F., & Zhou, H. M. (2001). *Biochimica et Biophysica Acta, 1545*, 305–313.
2. Zhang, Y. X., Zhu, Y., & Zhou, H. M. (2000). *The International Journal of Biochemistry & Cell Biology, 32*, 887–894. doi:10.1016/S1357-2725(00)00025-X.
3. Buck, M. (1998). *Quarterly Reviews of Biophysics, 31*, 297–355. doi:10.1017/S003358359800345X.
4. Deshusses, J. M., Burgess, J. A., Scherl, A., Wenger, Y., Walter, N., Converset, V., et al. (2003). *Proteomics, 3*, 1418–1424. doi:10.1002/pmic.200300492.
5. Wilkins, A. L., Yang, W., & Yang, J. J. (2003). *Current Protein & Peptide Science, 4*, 367–373. doi:10.2174/1389203033487063.
6. Buck, M., Radford, S. E., & Dobson, C. M. (1993). *Biochemistry, 32*, 669–678. doi:10.1021/bi00053a036.
7. Shiraki, K., Nishikawa, K., & Goto, Y. (1995). *Journal of Molecular Biology, 245*, 180–194. doi:10.1006/jmbi.1994.0015.
8. Yiu, C. P., Mateu, M. G., & Fersht, A. R. (2000). *ChemBioChem, 1*, 49–55. doi:10.1002/1439-7633(20000703)1:1<49::AID-CBIC49>3.0.CO;2-A.
9. Polverino de Laureto, P., Donadi, M., Scaramella, E., Frare, E., & Fontana, A. (2001). *Biochimica et Biophysica Acta, 1548*, 29–37.
10. Dubey, V. K., Shah, A., Jagannadham, M. V., & Kayastha, A. M. (2006). *Protein and Peptide Letters, 13*, 545–547. doi:10.2174/092986606777145823.
11. Hamada, D., Chiti, F., Guijarro, J. I., Kataoka, M., Taddei, N., & Dobson, C. M. (2000). *Nature Structural Biology, 7*, 58–61. doi:10.1038/71259.
12. Rezaei-Ghaleh, N., Ebrahim-Habibi, A., Moosavi-Movahedi, A. A., & Nemat-Gorgani, M. (2007). *International Journal of Biological Macromolecules, 41*, 597–604. doi:10.1016/j.ijbiomac.2007.07.018.
13. Rezaei-Ghaleh, N., Ebrahim-Habibi, A., Moosavi-Movahedi, A. A., & Nemat-Gorgani, M. (2007). *Archives of Biochemistry and Biophysics, 457*, 160–169. doi:10.1016/j.abb.2006.10.031.
14. Roccatano, D., Colombo, G., Fioroni, M., & Mark, A. E. (2002). *Proceedings of the National Academy of Sciences of the United States of America, 99*, 12179–12184. doi:10.1073/pnas.182199699.
15. Invernizzi, G., & Grandori, R. (2007). *Rapid Communications in Mass Spectrometry, 21*, 1049–1052. doi:10.1002/rcm.2940.
16. Soldi, G., Bemporad, F., Torrassa, S., Relini, A., Ramazzotti, M., Taddei, N., et al. (2005). *Biophysical Journal, 89*, 4234–4244. doi:10.1529/biophysj.105.067538.

17. Decker, H., & Tuczek, F. (2000). *Trends in Biochemical Sciences, 25*, 392–397. doi:10.1016/S0968-0004(00)01602-9.
18. Fenoll, L. G., Peñalver, M. J., Rodríguez-López, J. N., Varón, R., García-Cánovas, F., & Tudela, J. (2004). *The International Journal of Biochemistry & Cell Biology, 36*, 235–246. doi:10.1016/S1357-2725(03)00234-6.
19. Ray, K., Chaki, M., & Senqupta, M. (2007). *Progress in Retinal and Eye Research, 26*, 323–358. doi:10.1016/j.preteyeres.2007.01.001.
20. Gandía-Herrero, F., Jiménez, M., Cabanes, J., García-Carmona, F., & Escribano, J. (2003). *Journal of Agricultural and Food Chemistry, 51*, 7764–7769. doi:10.1021/jf030131u.
21. Guerrero, A., & Rosell, G. (2005). *Current Medicinal Chemistry, 12*, 461–469.
22. Park, Y. D., Kim, S. Y., Lyou, Y. J., Lee, J. Y., & Yang, J. M. (2005). *Biochimie, 87*, 931–937. doi:10.1016/j.biochi.2005.06.006.
23. Park, Y. D., Ou, W. B., Yu, T. W., & Zhou, H. M. (2001). *Biochemistry and Cell Biology, 79*, 479–487. doi:10.1139/bcb-79-4-479.
24. Zhao, T. J., Ou, W. B., Xie, Q., Liu, Y., Yan, Y. B., & Zhou, H. M. (2005). *The Journal of Biological Chemistry, 280*, 13470–13476. doi:10.1074/jbc.M413882200.
25. Han, H. Y., Zou, H. C., Jeon, J. Y., Wang, Y. J., Xu, W. A., Yang, J. M., et al. (2007). *Biochimica et Biophysica Acta, 1774*, 822–827.
26. Park, Y. D., Lee, S. J., Park, K. H., Kim, S. Y., Hahn, M. J., & Yang, J. M. (2003). *Journal of Protein Chemistry, 22*, 613–623. doi:10.1023/B:JOPC.0000008726.99095.48.
27. John, B., & Sali, A. (2003). *Nucleic Acids Research, 31*, 3982–3992. doi:10.1093/nar/gkg460.
28. Rodriguez, R., Chinea, G., Lopez, N., Pons, T., & Vriend, G. (1998). *Bioinformatics (Oxford, England), 14*, 523–528. doi:10.1093/bioinformatics/14.6.523.
29. Huey, R., Morris, G. M., Olson, A. J., & Goodsell, D. S. (2007). *Journal of Computational Chemistry, 28*, 1145–1152. doi:10.1002/jcc.20634.
30. Moustakas, D. T., Lang, P. T., Pegg, S., Pettersen, E., Kuntz, I. D., Brooijmans, N., et al. (2006). *Journal of Computer-Aided Molecular Design, 20*, 601–619. doi:10.1007/s10822-006-9060-4.
31. Xie, X. Q., & Chen, J. Z. J. (2008). *Chem Inf Model, 48*, 465–475. doi:10.1021/ci700193u.
32. Wei, X., Ding, S., Jiang, Y., Zeng, X. G., & Zhou, H. M. (2006). Biochemistry. *Biokhimiia, 71*, S77–S82. doi:10.1134/S000629790613013X.
33. Han, H. Y., Lee, J. R., Xu, W. A., Hahn, M. J., Yang, J. M., & Park, Y. D. (2007). *Journal of Biomolecular Structure & Dynamics, 25*, 165–171.
34. Park, Y. D., Lyou, Y. J., Hahn, H. S., Hahn, M. J., & Yang, J. M. (2006). *Journal of Biomolecular Structure & Dynamics, 24*, 131–138.
35. Park, K. H., Park, Y. D., Lee, J. R., Hahn, H. S., Lee, S. J., Bae, C. D., et al. (2005). *Biochimica et Biophysica Acta, 1726*, 115–120.
36. Park, Y. D., Jung, J. Y., Kim, D. W., Kim, W. S., Hahn, M. J., & Yang, J. M. (2003). *Journal of Protein Chemistry, 22*, 463–471. doi:10.1023/B:JOPC.0000005462.05642.89.
37. Tams, J. W., & Welinder, K. G. (1996). *Biochemistry, 35*, 7573–7579. doi:10.1021/bi953067l.